

Adaptive Enhancement and Dual-Pooling Sequential Attention for Lightweight Underwater Object Detection with YOLOv10

Md. Mushibur Rahman¹, Umme Fawzia Rahim², Enam Ahmed Taufik³

^{1,2}Department of Computer Science and Engineering, Dhaka University of Engineering & Technology
Gazipur, 1707, Bangladesh

³Department of Computer Science and Engineering, BRAC University
Dhaka, Bangladesh

¹mushiburrahman5@gmail.com, ²fawzia.rahim@duet.ac.bd, ³enam.ahmed.taufik@gmail.com

Abstract—Underwater object detection constitutes a pivotal endeavor within the realms of marine surveillance and autonomous underwater systems; however, it presents significant challenges due to pronounced visual impairments arising from phenomena such as light absorption, scattering, and diminished contrast. In response to these formidable challenges, this manuscript introduces a streamlined yet robust framework for underwater object detection, grounded in the YOLOv10 architecture. The proposed method integrates a Multi-Stage Adaptive Enhancement module to improve image quality, a Dual-Pooling Sequential Attention (DPSA) mechanism embedded into the backbone to strengthen multi-scale feature representation, and a Focal Generalized IoU Objectness (FGIoU) loss to jointly improve localization accuracy and objectness prediction under class imbalance. Comprehensive experimental evaluations conducted on the RUOD and DUO benchmark datasets substantiate that the proposed DPSA_FGIoU_YOLOv10n attains exceptional performance, achieving mean Average Precision (mAP) scores of 88.9% and 88.0% at IoU threshold 0.5, respectively. In comparison to the baseline YOLOv10n, this represents enhancements of 6.7% for RUOD and 6.2% for DUO, all while preserving a compact model architecture comprising merely 2.8M parameters. These findings validate that the proposed framework establishes an efficacious equilibrium among accuracy, robustness, and real-time operational efficiency, making it suitable for deployment in resource-constrained underwater settings.

Index Terms—Underwater object detection, YOLOv10, Image Enhancement, Attention Mechanism, Spatial Pyramid Pooling, FGIoU Loss, and Lightweight Deep Learning.

I. INTRODUCTION

Underwater object detection (UOD) is a foundational technology for marine ecological monitoring, autonomous subsea navigation, and intelligent resource management. However, underwater visual perception is inherently constrained by wavelength dependent absorption, scattering, and non-uniform illumination [1]. These optical phenomena induce color distortion, severe contrast degradation, and boundary blurring, which significantly compromise the reliability of detection models originally developed for terrestrial environments. The proliferation of deep learning has established convolutional neural network (CNN) based detectors as the standard paradigm for real-time visual perception. These architectures are deployed on re-

source constrained platforms, such as autonomous underwater vehicles (AUVs) and remotely operated vehicles (ROVs). This degradation stems from early-stage feature extraction failure due to poor image quality [2], as well as feature aggregation strategies and loss functions that do not adequately account for class imbalance and localization uncertainty.

Recent research efforts have sought to mitigate these challenges by integrating image enhancement, attention-based refinement, and specialized optimization objectives. Deterministic enhancement methods restore color fidelity and contrast, thereby stabilizing feature representations [3]. Furthermore, attention mechanisms improve robustness by prioritizing salient targets while suppressing environmental noise [4]. Advanced loss formulations, including Intersection-over-Union (IoU) variants and focal-weighted objectives, have also demonstrated utility in improving bounding box regression and mitigating foreground-background imbalance [5]. However, many existing methods rely on computationally intensive enhancement or heavy attention modules, limiting real-time deployment. The systematic integration of deterministic preprocessing, lightweight attention, and robust loss optimization remains underexplored.

In this work, we propose a lightweight and robust underwater object detection framework designed to enhance detection accuracy while preserving real-time efficiency. The primary contributions of this study can be summarized as follows:

- Introduce a Multi-Stage Adaptive Enhancement pipeline to correct color distortion, enhance contrast, and preserve structural details in degraded underwater images.
- We introduce a lightweight Dual-Pooling Sequential Attention mechanism that applies sequential channel and spatial attention to strengthen small object feature representation and suppress complex underwater backgrounds.
- We develop a hybrid loss function that jointly addresses class imbalance, improves bounding box localization, and enhances objectness calibration by integrating Focal Loss, Generalized IoU Loss, and Objectness Focal Loss.
- Comprehensive experiments on standard underwater benchmarks demonstrate consistent mAP improvements

while maintaining real-time inference performance suitable for embedded deployment.

II. RELATED WORK

The evolution of underwater object detection (UOD) is characterized by sustained efforts to address severe optical degradation, including wavelength-dependent absorption, backscattering, and the presence of small, densely packed targets. In Recent years, research has shifted toward end-to-end architectures optimized for real-time performance on resource-constrained hardware. Initial research focused on lightweight adaptations of the YOLO framework. For example, YOLO-UOD [6] adopted YOLOv7 as the baseline detector and achieved strong underwater detection performance on the URPC2018 dataset, reporting an mAP of 83.1% and an AP of 48.5% with 37.3M parameters, while maintaining efficient computational complexity. Along similar lines, CEH-YOLO [7] incorporated high-order deformable attention into YOLOv8, achieving 88.4% mAP on the DUO dataset and a detection speed of 156 FPS with only 4.4 M parameters. Similarly, Dynamic YOLO [8] enhanced detection sensitivity through deformable convolution v3 and achieved an mAP@.5 of 86.7% on the DUO dataset with 8.2 M parameters. These principles extend to sonar imagery, For instance, UWS-YOLO [9] achieved 87.1% mAP at 158 FPS by utilizing dynamic snake convolutions to model elongated structures. In Addition, SU-YOLO [10] introduced Spiking Neural Networks to achieve 78.8% mAP with an energy consumption of 2.98 mJ, demonstrating a path toward ultra-low power underwater sensing. Collectively, these advancements indicate a trajectory toward high-precision frameworks that balance multi-scale feature fusion with low computational complexity.

In addition to the YOLO architecture, alternative non-YOLO single-stage detectors have been explored for the purpose of underwater object detection. Building on SSD-based designs, jiang and Wang [11] incorporated shallow detection layers, weighted confidence loss, and MSRCR-based image enhancement, with an mAP of 66.9% on URPC2018, outperforming SSD, YOLOv3, and Faster R-CNN. Moving toward more advance one stage frameworks, Jia et al. [12] introduced an EfficientDet-based detector with enhanced channel interaction and multi-scale feature fusion, achieving 91.67% mAP on URPC and 92.81% mAP on a Kaggle dataset at 37.5 FPS. Similarly, Jain et al. [13] proposed DeepSeaNet, a modified EfficientDet model with BiSkFPN and multi-focal loss, attaining 98.63% mAP on the Brackish dataset. More recently, Jyothimurugan et al. [14] developed a DCGAN augmented YOLOv6 framework for Crown-of-Thorns Starfish detection on the CSIRO dataset, achieving 93.8% mAP@.5 with strong precision and recall while enabling real-time embedded deployment.

III. METHODOLOGY

A. Dataset

To enable fair comparison with existing methods, this study uses two established benchmark datasets for underwater object

detection: the RUOD dataset [15] and the DUO dataset [16]. The diversity in object categories, image resolutions, and class distributions makes these datasets suitable for evaluating robustness under challenging underwater conditions. The RUOD dataset consists of 9,340 images across 10 categories: fish, jellyfish, turtle, cuttlefish, diver, scallop, holothurian, coral, starfish, and echinus. All images are of size 640×640 pixels. The DUO dataset encompasses a total of 7,782 images across four categories: sea urchin, starfish, sea cucumber, and scallop. This dataset is characterized by images with five different resolutions: 3840×2160 , 1920×1080 , 720×405 , 586×480 , and 704×576 . The distribution of species categories within the two datasets are shown in Figure 1. RUOD and DUO are established benchmarks that cover diverse underwater object categories and imaging conditions.

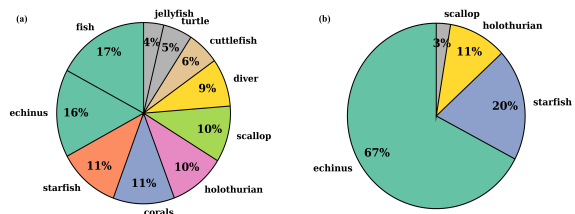


Fig. 1: Distribution of samples across object categories in the datasets: (a) RUOD dataset and (b) DUO dataset.

B. Multi-Stage Adaptive Preprocessing for Underwater Visual Perception

Underwater imaging is severely affected by wavelength-dependent attenuation and scattering, leading to color distortion, uneven illumination, and reduced contrast. In response to this issue, we proposed a Multi-Stage Adaptive Enhancement for Underwater Visual Perception (MAE-UVP) module implemented as a deterministic preprocessing framework. In Figure 2, the MAE-UVP comprises four sequential correction phases. (1) Adaptive color correction compensates for the dominant cyan bias through channel wise scaling to recover attenuated red components. (2) Luminance contrast Enhancement transitions the image into CIELAB color space and applies CLAHE exclusively to the luminance channel, thereby augmenting local contrast without introducing color distortion. (3) Soft-Guided Dehazing (SGD), employs a Gaussian-guided prior to delicately attenuate forward scattering haze while maintaining edge clarity and preventing halo artifacts. (4) Edge Preserving Refinement applies edge aware filtering to enhance object boundaries and reduce noise in homogeneous regions. MAE-UVP contains no learnable parameters, all hyperparameters are empirically determined and uses fixed, non-learnable hyperparameters to ensure deterministic, low-overhead, and reproducible enhancement.

C. Improved YOLOv10 Model Architecture

The proposed architectural builds upon the foundational YOLOv10 [17] framework by meticulously integrating a series

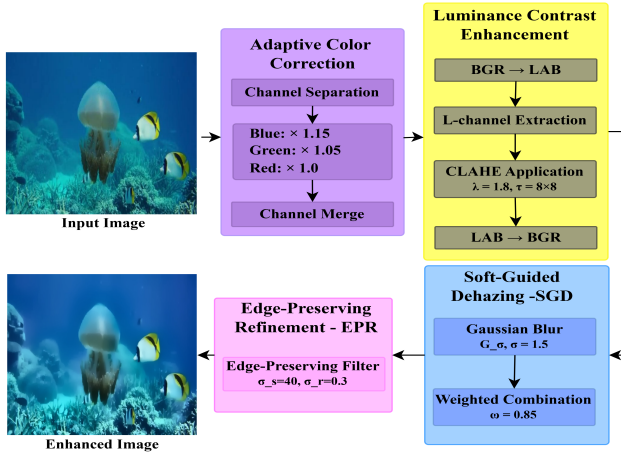


Fig. 2: Structure of MAE-UVP enhancement module.

of critical enhancements that are both innovative and functionally impactful. Specifically, the Spatial Pyramid Pooling Fast (SPPF) layer in the backbone is replaced with the proposed DPSA_SPPF module, which applies sequential channel and spatial attention to multi scale pooled features to enhance feature discrimination underwater conditions. This modification emphasizes salient object regions while suppressing background artifacts, without altering the backbone topology. In addition, the detection head is optimized by incorporating the proposed loss function, improving localization accuracy and objectness calibration. Notably, the PAN-FPN neck of YOLOv10 [17] remains unchanged, preserving the original feature aggregation strategy and ensuring fair comparison with the baseline. As shown in Figure 3, the architecture diagram highlights the backbone and head level modifications with the end-to-end, NMS-free detection pipeline.

D. Dual Pooling Sequential Attention (DPSA)

In the current investigation, the DPSA mechanism was judiciously integrated atop the SPPF layer of the backbone network, a design decision informed by two principal considerations. Firstly, this placement allows the multi-scale features generated by SPPF to sequential attention refinement, which helps suppress underwater noise and enhance object relevant representations. Secondly, computational efficiency is achieved by processing features post concatenation, capitalizing on DPSA streamlined structure while preventing redundant attention computations across scales.

The DPSA module consists of two sequential attention components with domain specific alterations. Channel Attention utilizes dual adaptive pooling processed through a shared two layer convolutional MLP with a fixed reduction ratio of sixteen, producing channel weights via sigmoid. Spatial Attention computes channel wise mean and maximum statistics, concatenates these, and applies a fixed 7×7 convolutional kernel with padding. The comprehensive DPSA processes features through channel attention followed by spatial attention. The DPSA_SPPF variant reduces channels via 1×1 convolution,

implements three parallel max pooling operations with kernels of 5×5 , 9×9 , and 13×13 , concatenates multi scale features, processing through DPSA, and concludes with a final 1×1 convolution, as shown in Figure 3. DPSA_SPPF balances feature enhancement with computational efficiency through post concatenation attention application, making it ideal for deployment scenarios demanding both accuracy and inference speed.

E. Focal Generalized IoU Objectness Loss (FGIoU Loss)

The FGIoU is a loss function designed for a sophisticated composite objective to comprehensively enhance the YOLOv10 detection Framework. This loss function amalgamates three distinct loss components specifically aimed at tackling fundamental issues: class imbalance, inaccurate localization, and poor objectness calibration. FGIoU Loss functions through a well structured pipeline commencing with the TaskAlignedAssigner, which aligns predictions from the dual detection heads of YOLOv10 with corresponding ground truth annotations, subsequently followed by the simultaneous computation of losses and their weighted aggregation. The overall formulation of FGIoU Loss is articulated as:

$$\mathcal{L}_{FGIoU} = 7.5 \cdot \mathcal{L}_{GIoU} + 0.5 \cdot \mathcal{L}_{Focal} + 1.0 \cdot \mathcal{L}_{ObjFocal} \quad (1)$$

The loss weights were selected via preliminary experiments and remain stable under small ($\pm 20\%$) variations. Where coefficients are meticulously calibrated to prioritize the precision of bounding boxes while simultaneously balancing contributions from classification and objectness.

- Generalized IoU Loss refines the process of bounding box regression by imposing penalties for both insufficient overlap and spatial separation:

$$\mathcal{L}_{GIoU} = 1 - \left(\text{IoU} - \frac{|C \setminus (A \cup B)|}{|C|} \right) \quad (2)$$

Where A and B are predicted and ground truth boxes and c is their minimal enclosing convex hull.

- Focal Loss addresses the imbalance between foreground and background by concentrating the training process on challenging examples:

$$\mathcal{L}_{Focal}(p_t) = -\alpha(1 - p_t)^\gamma \log(p_t) \quad (3)$$

Here, p_t is the predicted class probability, α balances class weight, and γ controls the focusing intensity.

- Objectness Focal Loss enhances the calibration of confidence through the application of focal weighted binary cross entropy:

$$\mathcal{L}_{ObjFocal}(p_t) = \alpha(1 - p_t)^\gamma \cdot \text{BCE}(p_t, t) \quad (4)$$

where p_t is the objectness score and $t \in \{0, 1\}$ is the ground-truth label.

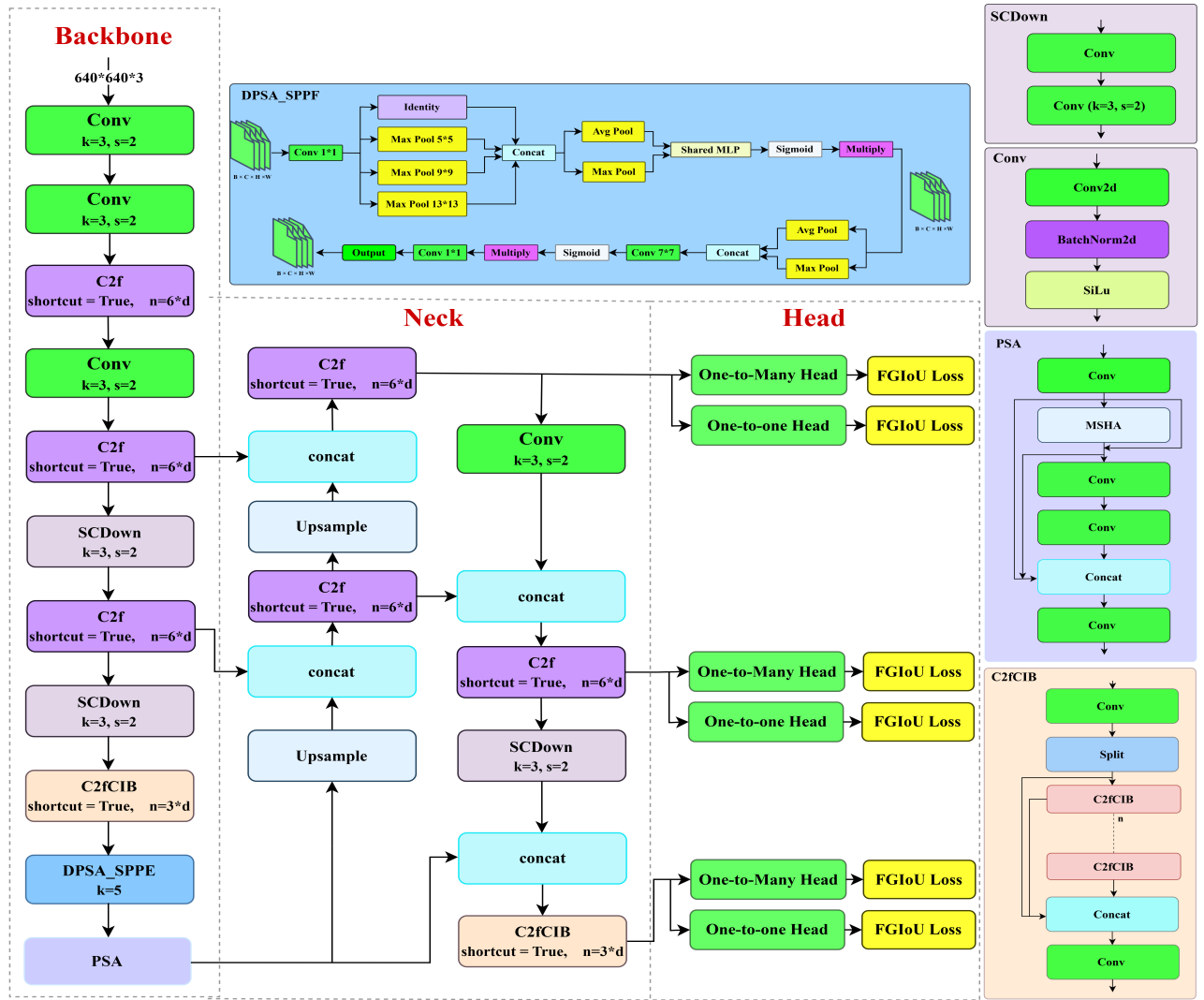


Fig. 3: Proposed YOLOv10 architecture with SPPF replaced by DPSA_SPPF in the backbone and modified detection head.

F. Model Evaluation Metrics

In this experiment, five metrics are employed to evaluate the detection performance of the proposed YOLOv10 model in the context of underwater object detection. The respective formulas are articulated in equations (5)-(9), encompassing Precision, Recall, Average Precision (AP), Mean Average Precision (mAP), and F1 score.

$$\text{Precision} = \frac{TP}{TP + FP} \times 100\% \quad (5)$$

$$\text{Recall} = \frac{TP}{TP + FN} \times 100\% \quad (6)$$

$$AP = \int_0^1 P(R) dR \quad (7)$$

$$mAP = \frac{\sum_{j=1}^c (AP)_j}{c} \quad (8)$$

$$F1\text{-score} = 2 \times \frac{\text{Precision} \times \text{Recall}}{\text{Precision} + \text{Recall}} \quad (9)$$

Where TP denotes true positives, FP signifies false positives, and FN indicates false negatives. Precision measures the model's capability to differentiate negative samples, with higher values indicating superior accuracy in positive predictions. Higher recall denotes a greater proportion of correctly identified positive samples by the model. The F1 score integrates both metrics, with elevated values reflecting a more robust model. The variable C in Equation (7) represents the number of classes evaluated, which was four in this study. For mAP50 calculation, and IoU threshold of 0.5 indicates that model predictions are deemed correct when the intersection over union exceeds 0.5. The F1 score serves to provide a holistic assessment of model performance in instances of significant disparity between accuracy and recall.

G. Experimental Setup

Experimental procedures were executed utilizing PyTorch 2.x on the Kaggle platform, augmented by GPU acceleration via (Tesla P100). All models were trained for 100 epochs utilizing a 640×640 input resolution and a batch size of 16. The AdamW optimizer was employed with an initial learning rate of 0.01, scheduled using cosine decay, a momentum coefficient of 0.937, and a weight decay of 0.0005. Furthermore, early stopping was instituted with a patience of 10 epochs to alleviate the risk of overfitting. The model achieves an average inference time of 2.1 ms per image (approximately 476 FPS) at 640×640 resolution.

IV. RESULTS AND DISCUSSION

The section presents the experimental evaluation of model enhancements, beginning with an ablation study conducted on the baseline YOLOv10n [17] model to assess the contributions of the DPSA_SPPF module and FGIoU loss. The proposed method is compared with existing YOLO variants on the RUOD and DUO datasets, highlighting its impact on detection accuracy, precision, and robustness in complex underwater environments. Due to space limitations, only overall metrics are reported, while consistent PR trends are observed.

TABLE I: Experimental comparison with the baseline model.

Dataset	Method	DPSA_SPPF	FGIoU Loss	mAP50 (%)	mAP50:95 (%)
RUOD	YOLOv10n	–	–	82.2	58.8
	YOLOv10n	Yes	–	88.3 (+6.1)	65.1 (+6.3)
	YOLOv10n	–	Yes	88.0 (+5.8)	64.9 (+6.1)
	YOLOv10n	Yes	Yes	88.9 (+6.7)	66.5 (+7.7)
DUO	YOLOv10n	–	–	81.8	63.5
	YOLOv10n	Yes	–	85.7 (+3.9)	66.4 (+2.9)
	YOLOv10n	–	Yes	87.4 (+5.6)	68.0 (+4.5)
	YOLOv10n	Yes	Yes	88.0 (+6.2)	69.1 (+5.6)

A. Component Wise Impact Analysis of Model Enhancements

Table I presents a component-wise ablation analysis evaluating the individual and combined effects of the DPSA_SPPF module and the FGIoU loss on the baseline YOLOv10n model across the RUOD and DUO datasets. On the RUOD dataset, the baseline model achieves an mAP@0.5 of 82.2% and an mAP@0.5:0.95 of 58.8%. Introducing the DPSA_SPPF module alone improves feature representation, increasing mAP@0.5 to 88.3% (+6.1%) and mAP@0.5:0.95 to 65.1% (+6.3%). Replacing the conventional loss function with FGIoU enhances localization accuracy, resulting in mAP@0.5 and mAP@0.5:0.95 scores of 88.0% (+5.8%) and 64.9% (+6.1%), respectively. The joint application of both enhancements yields optimal performance, achieving an mAP@0.5 of 88.9% and an mAP@0.5:0.95 of 66.5%. Compared with the baseline, this corresponds to gains of +6.7% and +7.7%, respectively. Consistent trends are observed on the DUO dataset, where the baseline mAP@0.5 and mAP@0.5:0.95 scores of 81.8% and 63.5% are improved to 85.7% (+3.9%) and 66.4% (+2.9%) with DPSA_SPPF, and to 87.4% (+5.6%) and 68.0% (+4.5%) with FGIoU. The combined approach achieves optimal performance with mAP@0.5 and mAP@0.5:0.95 scores of 88.0% and 69.1%, indicating enhancements of +6.2% and +5.6%

over the baseline. These results demonstrate that the proposed architectural attention enhancement and loss optimization provide complementary benefits, yielding consistent and significant performance improvements across both datasets while preserving the lightweight nature of the baseline model.

B. Comparative Evaluation with State-of-the-Art Models

Table II compares the proposed DPSA_FGIoU_YOLOv10n model in comparison to leading YOLO variants, which encompass YOLOv8 (n, s, m), YOLO9t, YOLOv10 (n, s), and YOLOv11n, utilizing the RUOD and DUO datasets. Within the RUOD dataset, the proposed model shows the highest level of detection efficacy, achieving 86.7% precision, 82.1% recall, 88.9% mAP@0.5 (± 0.3 over three runs), 66.5% mAP@0.5-0.95, thereby surpassing YOLOv10n (82.3% precision, 76.0% recall, 82.2% mAP@0.5) and the YOLOv8 variants, which exhibit a lower overall mAP despite their competitive precision metrics. Conversely, on the DUO dataset, although YOLOv10n displays marginally elevated 88.3% precision, the proposed model secures superior 78.6% recall and mAP metrics (88.0% mAP@0.5 (± 0.3 over three runs), 69.1% mAP@0.5-0.95), thereby showing a more balanced and reliable capability for object detection in challenging underwater environments. Notably, the proposed model maintains a lightweight architecture with only 2.8M parameters, which is substantially smaller than YOLOv8s and YOLOv8m, demonstrating an effective trade-off between detection performance and computational efficiency. These results highlight the superiority of DPSA_FGIoU_YOLOv10n for real-time underwater object detection under resource-constrained conditions.

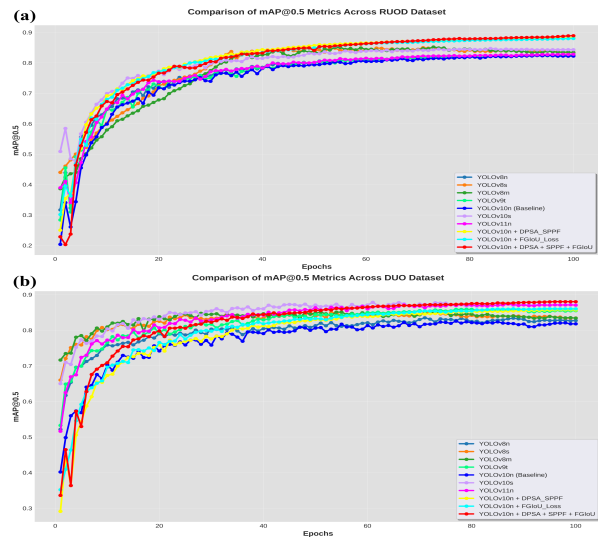


Fig. 4: Comparison of mAP@0.5 Metrics Across (a) RUOD, and (b) DUO dataset.

C. In Depth Analysis of Model Performance Across Datasets

Figure 4 presents a detailed comparison of mean Average Precision (mAP@.5) metrics for the RUOD and DUO

TABLE II: Comparison of the improved YOLOv10n variants with state-of-the-art methods for underwater object detection on the RUOD and DUO datasets

Model	RUOD Dataset				DUO Dataset				Parameters
	Prec. %	Rec. %	mAP@0.5 %	mAP@0.5-0.95 %	Prec. %	Rec. %	mAP@0.5 %	mAP@0.5-0.95 %	
YOLOv8n	83.8	75.0	82.6	58.4	81.9	75.7	82.7	64.1	3.1M
YOLOv8s	85.7	78.5	85.6	61.4	86.5	76.7	83.4	67.0	11.1M
YOLOv8m	85.6	77.9	85.8	62.1	85.7	76.8	83.4	68.4	25.8M
YOLOv9t	84.1	75.1	82.4	59.0	86.5	77.6	85.5	66.4	2.01M
YOLOv10n	82.3	76.0	82.2	58.8	88.3	68.4	81.8	63.5	2.7M
YOLOv10s	84.4	78.2	84.3	61.9	84.6	78.5	86.1	66.3	8.1M
YOLOv11n	83.2	76.5	82.8	58.8	84.0	77.6	85.8	66.7	2.60M
Dynamic YOLO [8]	-	-	-	-	-	-	86.7	68.6	8.2M
DPSA_YOLOv10n (Ours)	85.7	80.7	88.3	65.1	84.5	78.2	85.7	66.4	2.728M
FGIoU_YOLOv10n (Ours)	85.7	80.5	88.0	64.9	87.1	78.0	87.4	68.0	2.77M
DPSA_FGIoU_YOLOv10n (Ours)	86.7	82.1	88.9	66.5	87.2	78.6	88.0	69.1	2.8M

datasets. The plots demonstrate the performance trajectories of various YOLO variants across epochs, particularly highlighting the proposed DPSA_FGIoU_YOLOv10n model. The DPSA_FGIoU_YOLOv10n model consistently surpasses the baseline YOLOv10n in mAP@0.5 across both datasets, with improved values at every epoch. The incorporation of the DPSA_SPPF attention module and FGIoU loss function significantly enhances model performance, facilitating a continuous increase in mAP scores during training. Conversely, although YOLOv8 variants exhibit competitive precision, they are less consistent and overall inferior to the DPSA_FGIoU_YOLOv10n model. The findings highlight the benefits of the proposed architectural enhancements, showcasing the model’s capacity for high detection accuracy and strong performance, thus rendering it suitable for practical applications necessitating precision and computational efficiency.

V. CONCLUSION

This paper presented an efficient and lightweight underwater object detection framework built upon YOLOv10 to address challenges arising from underwater visual degradation and small object detection. By incorporating a deterministic Multi-Stage Adaptive Enhancement preprocessing pipeline, the Dual-Pooling Sequential Attention mechanism and FGIoU loss enhance feature representation, localization accuracy, and objectness calibration while maintaining computational efficiency. Experimental findings on the RUOD and DUO datasets reveal substantial and consistent advancements compared to the baseline YOLOv10n, achieving absolute mAP@0.5 gains of up to 6.7% and 6.2%, respectively, while preserving a compact architecture with only 2.8M parameters. These improvements stem from the complementary effects of attention based feature refinement and loss level optimization. Overall, the proposed framework provides a practical and reliable solution for real-time underwater perception on embedded platforms and also explore temporal feature modeling and domain adaptation to further enhance robustness in dynamic underwater environments.

REFERENCES

[1] D. Akkaynak and T. Treibitz, “A revised underwater image formation model,” *Proceedings of the IEEE Conference on Computer Vision and Pattern Recognition*, pp. 6723–6732, 2018.

[2] C. Li, C. Guo, W. Ren, R. Cong, J. Hou, S. Kwong, and D. Tao, “Underwater image processing: A comprehensive review,” *IEEE Transactions on Circuits and Systems for Video Technology*, vol. 29, no. 3, pp. 712–728, 2019.

[3] M. J. Islam, Y. Xia, and J. Sattar, “Fast underwater image enhancement for improved visual perception,” *IEEE robotics and automation letters*, vol. 5, no. 2, pp. 3227–3234, 2020.

[4] S. Woo, J. Park, J.-Y. Lee, and I. S. Kweon, “Cbam: Convolutional block attention module,” in *Proceedings of the European Conference on Computer Vision*, 2018, pp. 3–19.

[5] H. Rezaatofghi, N. Tsoi, J. Gwak, A. Sadeghian, I. Reid, and S. Savarese, “Generalized intersection over union: A metric and a loss for bounding box regression,” *Proceedings of the IEEE Conference on Computer Vision and Pattern Recognition*, pp. 658–666, 2019.

[6] W. Chen, T. Zhuang, Y. Zhang, T. Mei, and X. Tang, “Yolo-uod: An underwater small object detector via improved efficient layer aggregation network,” *IET Image Processing*, vol. 18, no. 9, pp. 2490–2505, 2024.

[7] J. Feng and J. Tao, “Ceh-yolo: A composite enhanced yolo-based model for underwater object detection,” *Ecological Informatics*, vol. 82, p. 102758, 2024.

[8] J. Chen and M. J. Er, “Dynamic yolo for small underwater object detection,” *Artificial Intelligence Review*, vol. 57, no. 6, p. 165, 2024. [Online]. Available: <https://doi.org/10.1007/s10462-024-10788-1>

[9] L. Zhao, X. Ren, L. Fu, Q. Yun, and J. Yang, “Uws-yolo: Advancing underwater sonar object detection via transfer learning and orthogonal-snake convolution mechanisms,” *Journal of Marine Science and Engineering*, vol. 13, no. 10, 2025. [Online]. Available: <https://www.mdpi.com/2077-1312/13/10/1847>

[10] C. Li, W. Liu, G. Gong, X. Ding, and X. Zhong, “Su-yolo: Spiking neural network for efficient underwater object detection,” 2025. [Online]. Available: <https://arxiv.org/abs/2503.24389>

[11] Z. Jiang and R. Wang, “Underwater object detection based on improved single shot multibox detector,” in *Proceedings of the 2020 3rd International Conference on Algorithms, Computing and Artificial Intelligence*, 2020, pp. 1–7.

[12] J. Jia, M. Fu, X. Liu, and B. Zheng, “Underwater object detection based on improved efficientdet,” *Remote Sensing*, vol. 14, no. 18, p. 4487, 2022.

[13] S. Jain, “Deepseanet: Improving underwater object detection using efficientdet,” in *2024 4th International Conference on Applied Artificial Intelligence (ICAAI)*. IEEE, 2024, pp. 1–11.

[14] M. Jyothimurugan, S. Pavithra, and J. Deepika Roselind, “Efficient underwater ecological monitoring with embedded ai: detecting crown-of-thorns starfish via dgan and yolov6,” *Frontiers in Marine Science*, vol. 12, p. 1658205, 2025.

[15] Cttlab, “Ruod dataset,” <https://universe.roboflow.com/cttlab/ruod-copy>, dec 2023, visited on 2025-9-20. [Online]. Available: <https://universe.roboflow.com/cttlab/ruod-copy>

[16] C. Liu, H. Li, S. Wang, M. Zhu, D. Wang, X. Fan, and Z. Wang, “A dataset and benchmark of underwater object detection for robot picking,” in *2021 IEEE international conference on multimedia & expo workshops (ICMEW)*. IEEE, 2021, pp. 1–6.

[17] A. Wang, H. Chen, L. Liu, K. Chen, Z. Lin, J. Han *et al.*, “Yolov10: Real-time end-to-end object detection,” *Advances in Neural Information Processing Systems*, vol. 37, pp. 107984–108011, 2024.